Supplementary data

PTEN-null Tumors Cohabiting the Same Lung Display Differential Akt Activation and Sensitivity to Dietary Restriction

Natasha L. Curry[1], Mari Mino-Kenudson[3], Trudy G. Oliver[4†], Ömer H. Yilmaz[3,6], Vedat O. Yilmaz[1], Jade Y. Moon[1], Tyler Jacks[4], David M. Sabatini[4,5,6] & Nada Y. Kalaany[1,2*]

Author Affiliations:

[1]Division of Endocrinology, Center for Basic and Translational Obesity Research, Boston Children's Hospital, Boston, MA 02115

[2]Department of Pediatrics, Harvard Medical School, Boston, MA 02115

[3]Department of Pathology, Massachusetts General Hospital and Harvard Medical School, Boston, MA 02114

[4]Howard Hughes Medical Institute and Department of Biology, Massachusetts Institute of Technology; The David H. Koch Institute for Integrative Cancer Research at MIT, Cambridge, MA 02139

[5]Broad Institute of Harvard and MIT, Cambridge, MA 02142

[6]Whitehead Institute for Biomedical Research, Cambridge, MA 02142

[†]Present address: Department of Oncological Sciences, University of Utah and Huntsman Cancer Institute, Salt Lake City, UT 84112

[*]To whom correspondence may be addressed. Email: nada.kalaany@childrens.harvard.edu

Content

Supplementary Figures

The Supplementary figures (Figs. S1-S11) provide additional characterization of the KPTEN, Kp53 and KPTENp53 mouse models of lung cancer, the alveolar and bronchiolar tumors they harbor, and the cells derived from these tumors.

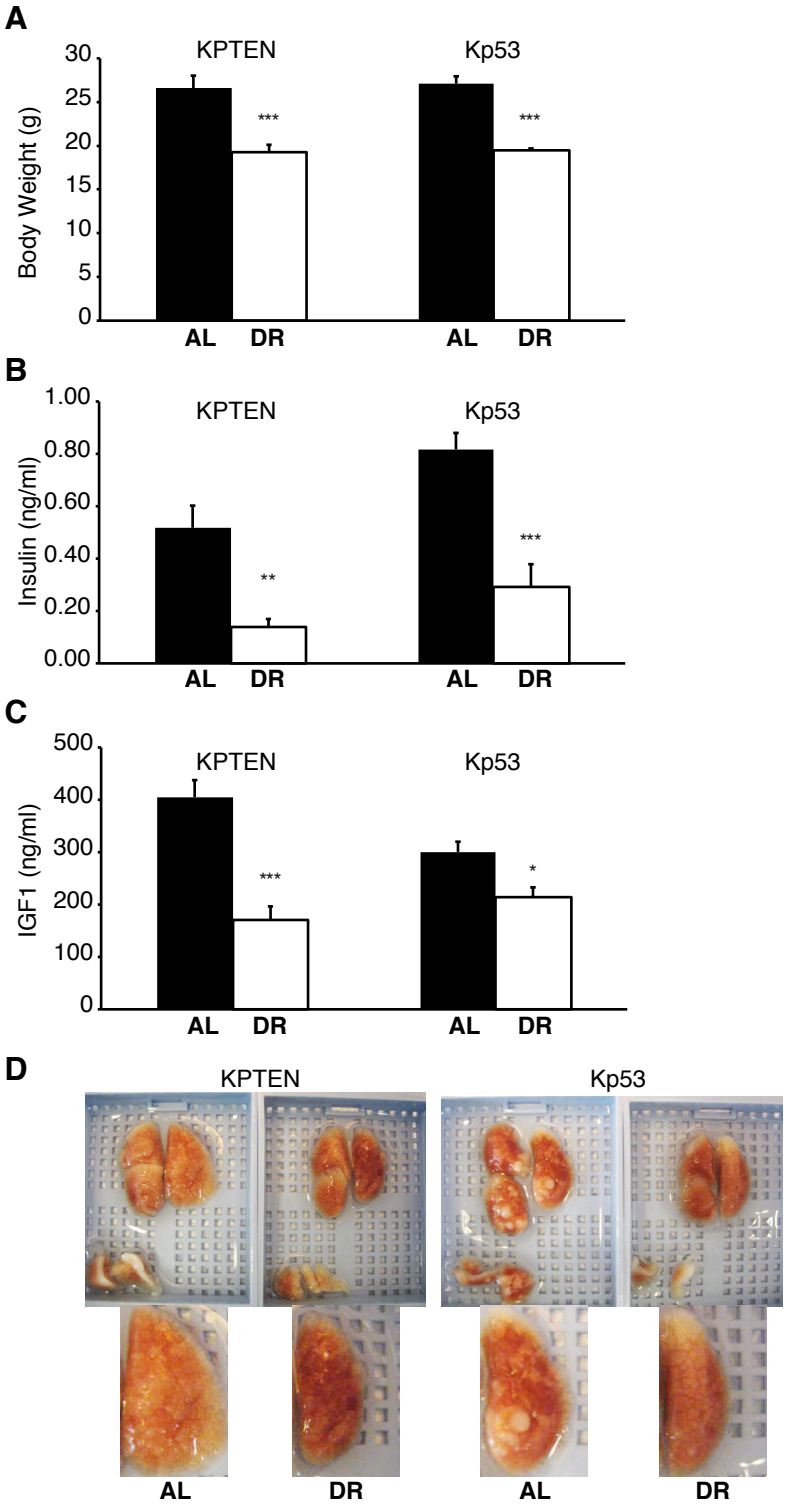

Figure S1: Body weights and plasma insulin and IGFI levels of KPTEN and Kp53 mice under AL and DR conditions. A-C, Body weights (**A**), plasma insulin (**B**), and plasma IGF1 (**C**) of *ad-libitum*-fed (AL) and dietary restricted (DR) KPTEN and Kp53 mice at the end of the dietary restriction studies. All DR groups had similar body weights to their AL counterparts at the beginning of the experiments, (n=5-7 mice). Values are means ± SEM. *$P < 0.05$; **$P < 0.01$; ***$P < 0.001$. **D**, Images of representative lung lobes (upper panel) from KPTEN and Kp53 mice showing decreased tumor burden under DR (versus AL) conditions. Lower panel images are a 2x magnification of the left lung shown in the upper panel. Note that KPTEN mice present with lung surface nodules that are smaller but more numerous than those observed in Kp53 mice.

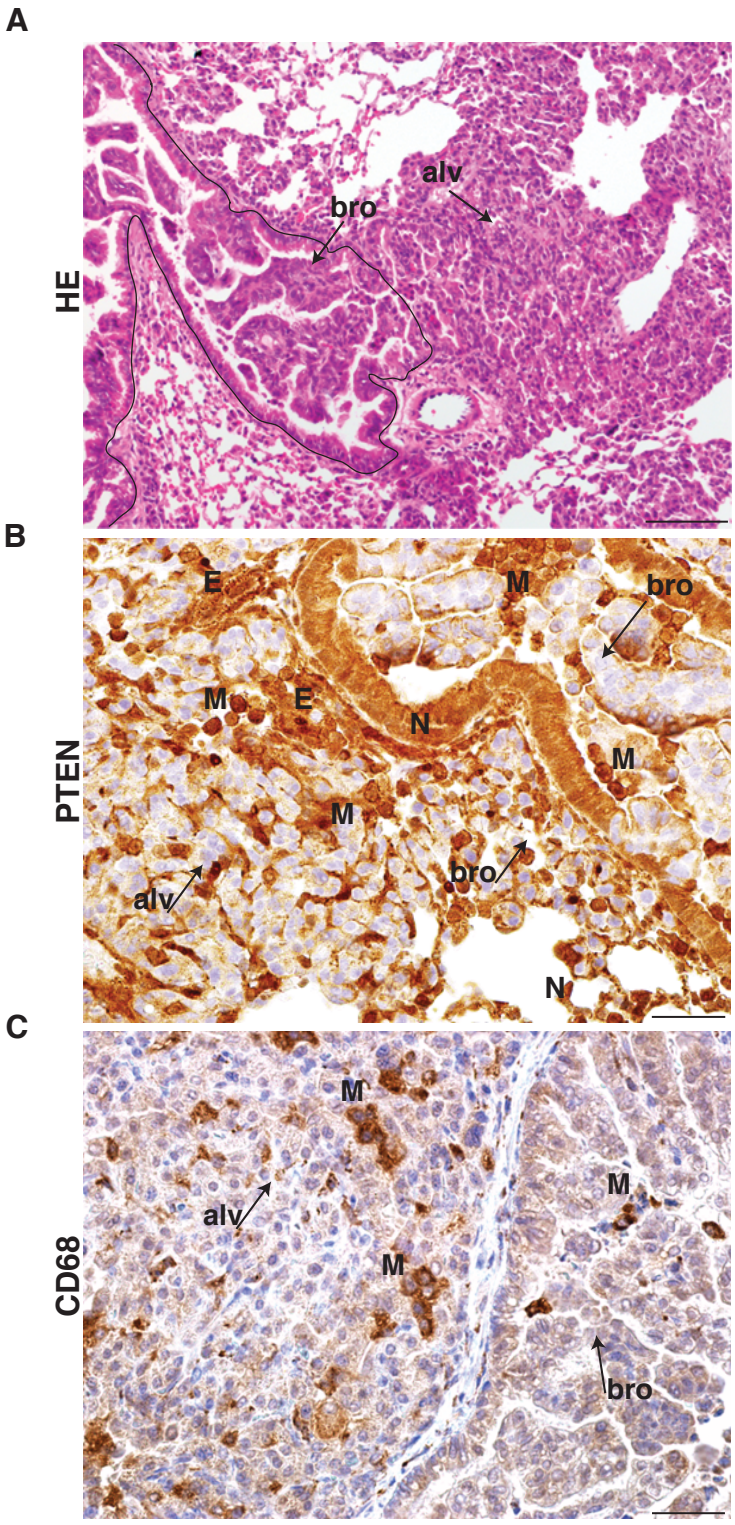

Figure S2: KPTEN bronchiolar and alveolar tumor cells display PTEN loss. A-C, H&E staining (**A**) and immunohistochemical analyses of PTEN (**B**), and CD68 (**C**) in sections of lungs from KPTEN mice under *ad-libitum* conditions. Arrows indicate alveolar (alv) or bronchiolar (bro) tumors; M: macrophages; N: normal cells; E: endothelial cells. Scale bars, 40 μm. The black line in (**A**) marks the outside layer of a tumor-enclosing bronchiole.

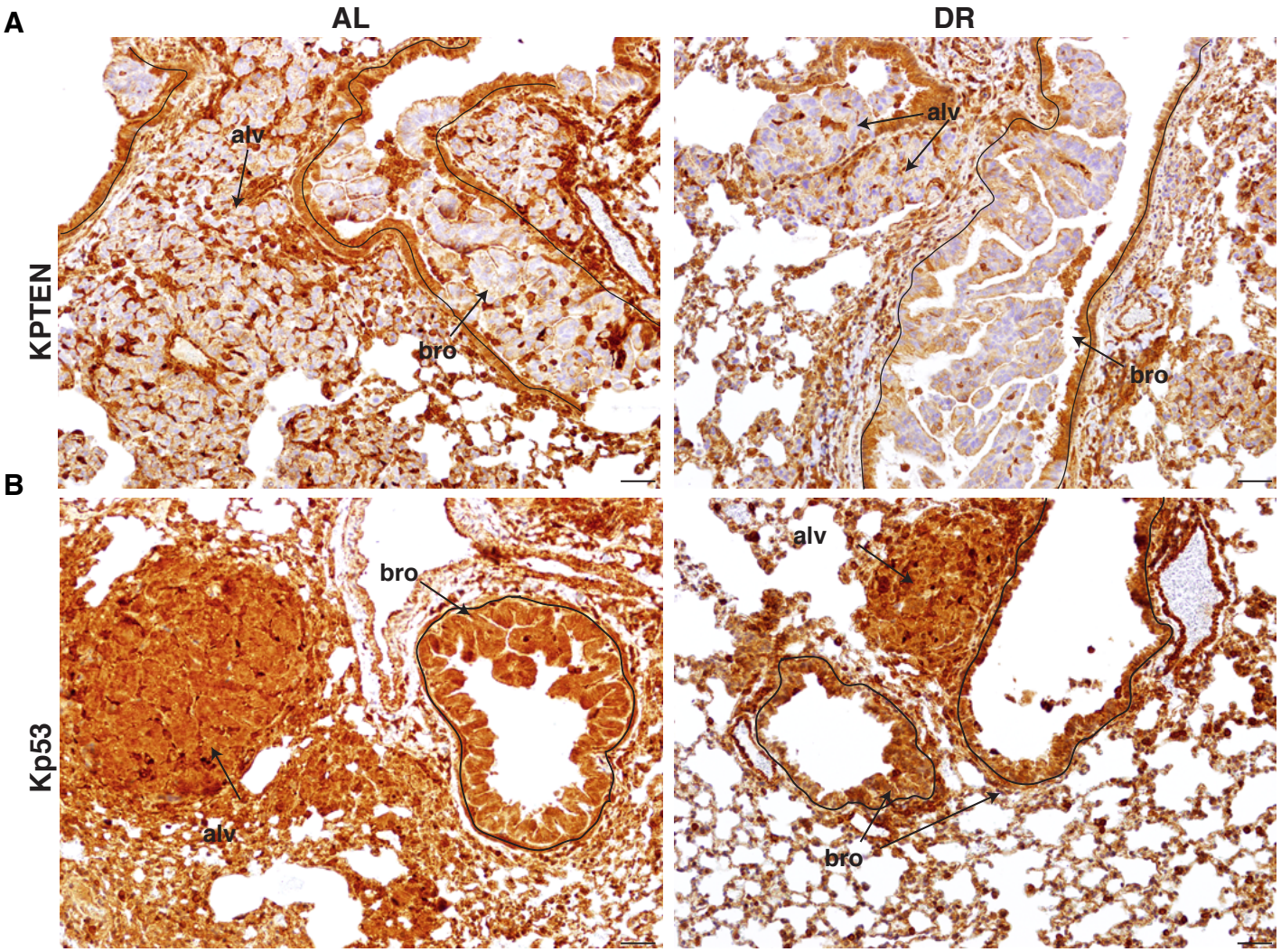

Figure S3: PTEN is expressed in Kp53 but not KPTEN alveolar and bronchiolar tumors.
A and **B**, Immunohistochemical analysis of PTEN in lungs from KPTEN (**A**) and Kp53 (**B**) mice under *ad-libitum* (AL) or DR conditions. Arrows indicate alveolar (alv) or bronchiolar (bro) tumors. All pictures were taken under the same magnification; scale bars, 40 μm. The black line marks the outside layer of tumor-enclosing bronchioles.

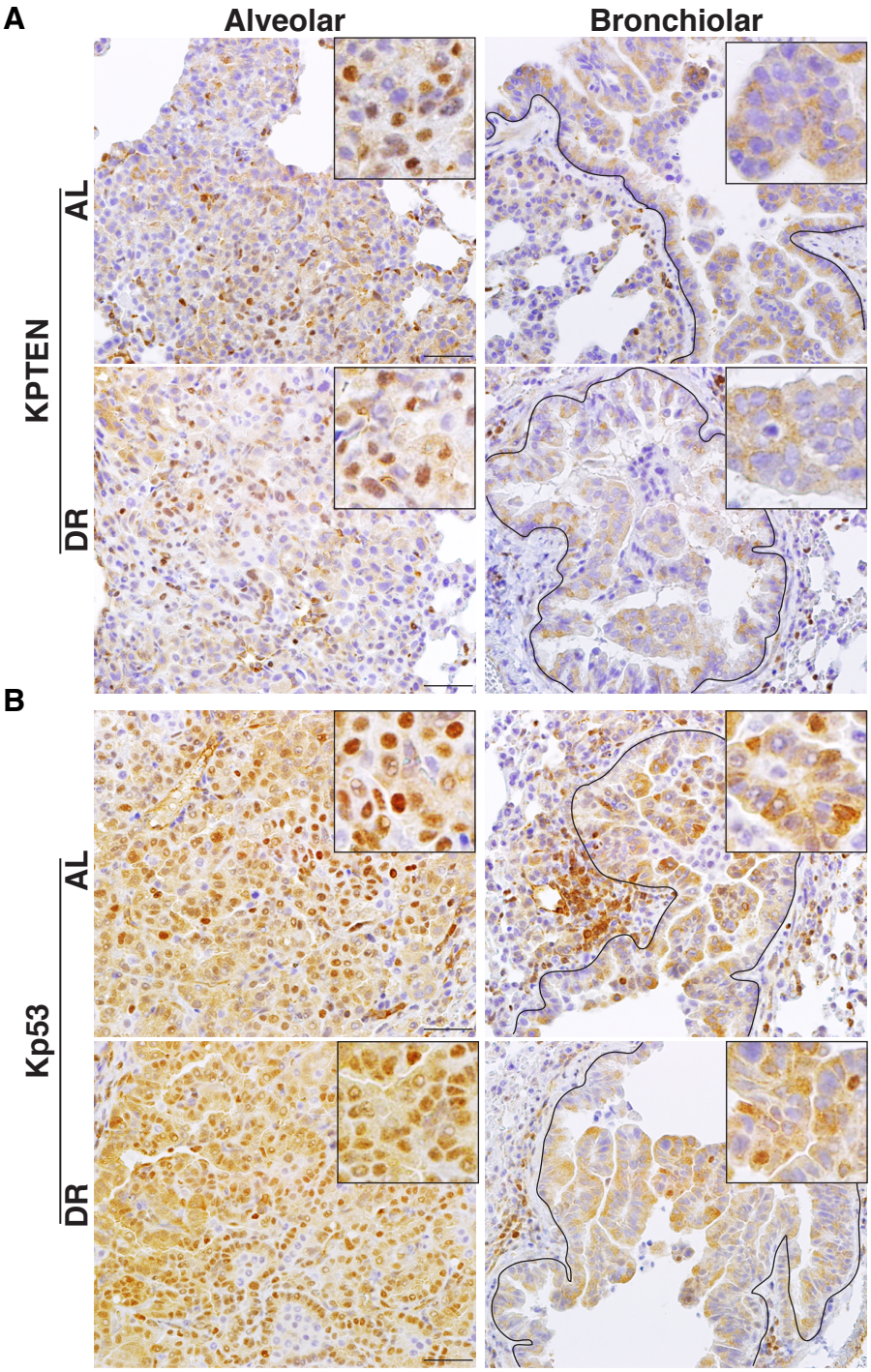

Figure S4: Differential FOXO1 cellular localization in KPTEN and Kp53 tumors.
A and **B**, Immunohistochemical analysis of FOXO1 in lungs from KPTEN (**A**) and Kp53 (**B**) mice under *ad-libitum* (AL) or DR conditions. Note the presence of nuclear FOXO1 in alveolar (**A**, left) but not bronchiolar (**A**, right) tumors of KPTEN mice and its presence, to a larger extent, in alveolar tumors of Kp53 mice (**B**, left), under AL or DR conditions. FOXO1 is mostly cytoplasmic in bronchiolar tumors of KPTEN mice (**A**, right), but is present in the nuclei of bronchiolar tumor cells of Kp53 mice (**B**, right). All pictures were taken under the same magnification; scale bars, 40 μm. Framed insets are a 2.2-fold magnification of a representative alveolar (left) or bronchiolar (right) tumor area. The black line in the right column marks the outside layer of tumor-enclosing bronchioles.

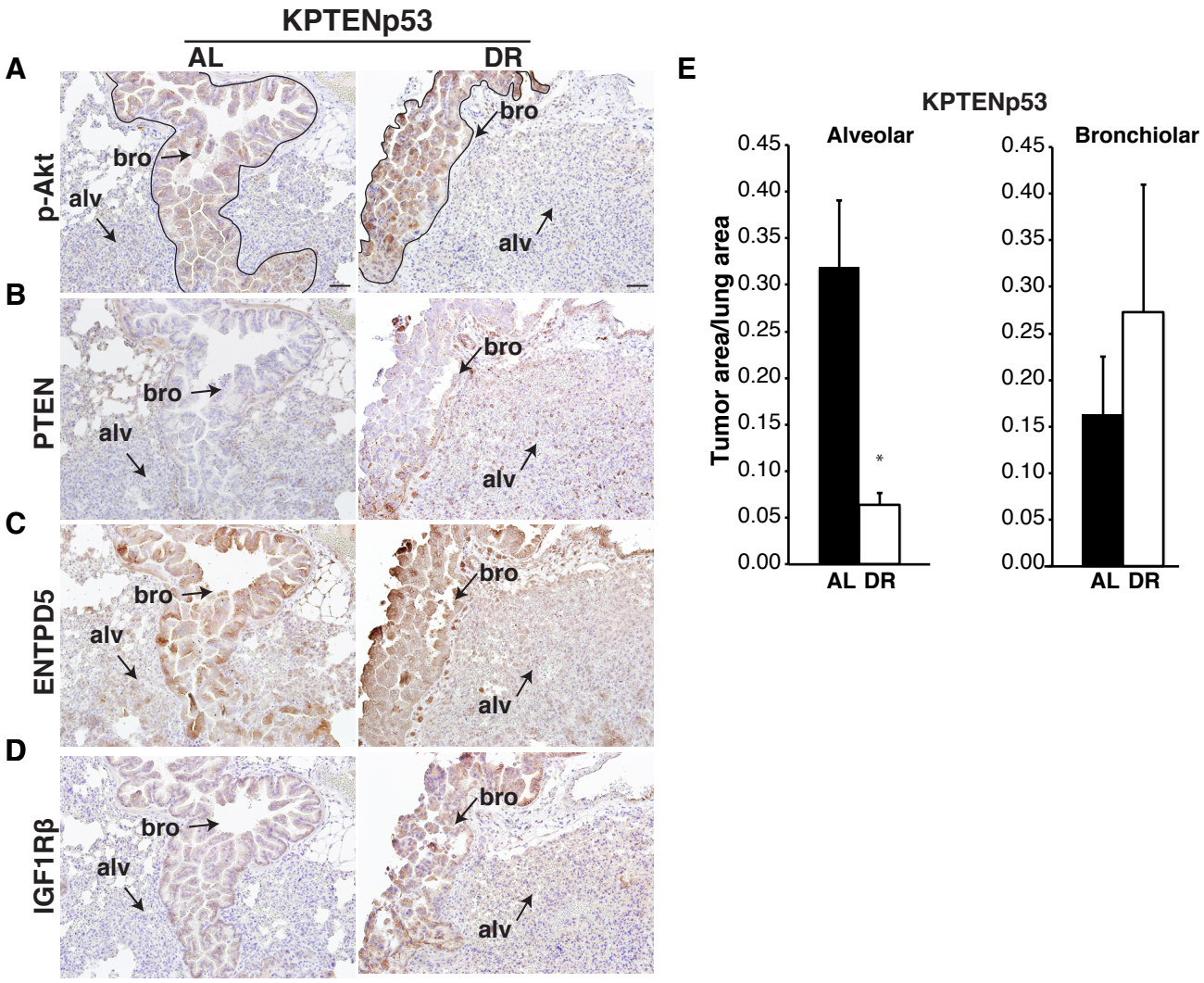

Figure S5: KPTENp53 bronchiolar and alveolar tumors display a phenotype similar to that of KPTEN tumors. A-D, Immunohistochemical analyses of phospho-S473 Akt (**A**), PTEN (**B**), ENTPD5 (**C**) and IGF1Rβ (**D**) in sequential sections of lungs from KPTENp53 mice under *ad-libitum* (AL) or DR conditions. **E**, Alveolar and bronchiolar tumor burden, measured by the ratio of tumor area over lung area in KPTENp53 mice that have been either AL-fed or underwent DR for 3 weeks (n=3 mice). In (**A-D**), arrows indicate alveolar (alv) or bronchiolar (bro) tumors. All pictures were taken under the same magnification; scale bars, 50 μm. The black line in (**A**) marks the outside layer of tumor-enclosing bronchioles. In (**E**), data are means ± S.E.M. **P* < 0.05.

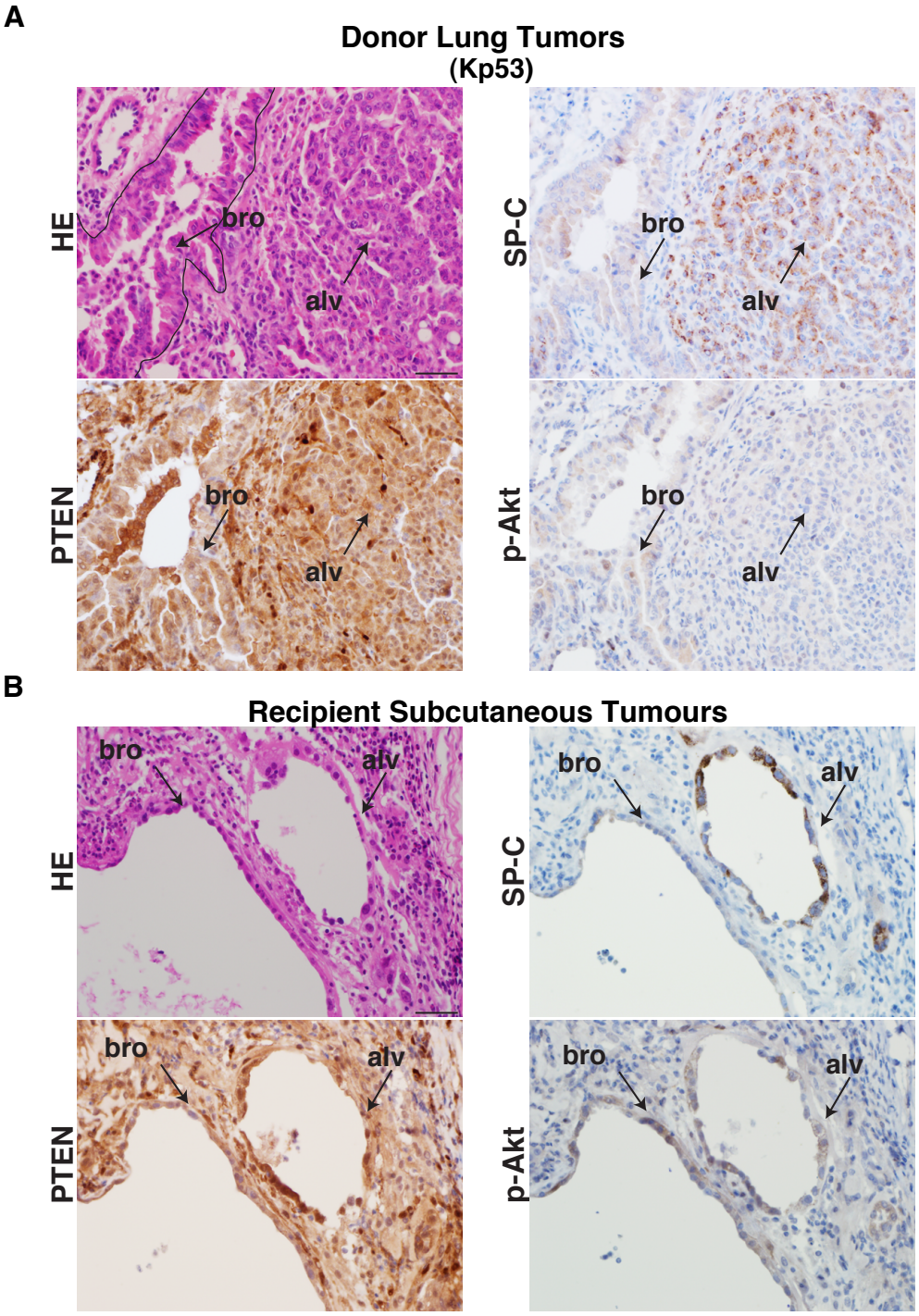

Figure S6: The alveolar and bronchiolar tumor phenotype of low Akt activity in Kp53 mice is maintained upon transplantation from donor to recipient mice. A and **B**, H&E staining and immunohistochemical analyses of SPC, PTEN, and phospho-S473 Akt in the lungs of a Kp53 donor mouse (**A**) and in subcutaneous tumors of a Kp53 recipient mouse (**B**), 24 days following injection of 10^6 donor tumor cells. Arrows indicate alveolar (alv) or bronchiolar (bro) tumors. All pictures were taken under the same magnification; scale bars, 40 μm. The black line in (**A**) marks the outside layer of a tumor-enclosing bronchiole.

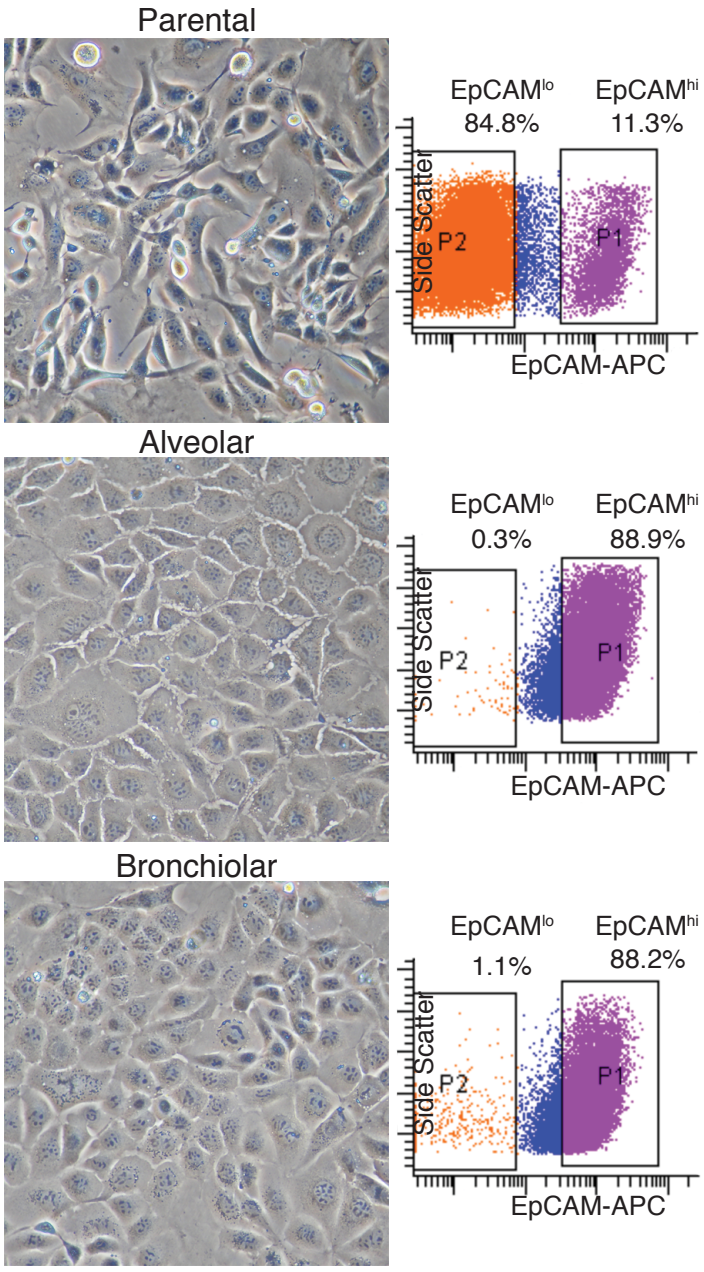

Figure S7: Alveolar and bronchiolar tumor cells isolated from KPTENp53 mice have epithelial characteristics. Representative pictures of parental, bronchiolar and alveolar cell lines passaged at least five times in culture plates *in vitro* (left panels) and corresponding flow cytometry graphs (right panels) demonstrating the epithelial enrichment ($EpCAM^{hi}$, population P1) of alveolar (88.9%) and bronchiolar (88.2%) cell lines isolated from the parental cells (P1, 11.3%). Loss of the non-epithelial ($EpCAM^{lo}$) cell population P2 in alveolar (0.3%) and bronchiolar (1.1%) cell lines is also depicted compared to the parental cells (84.8%). Dead cells were excluded from the analysis with the viability dye 7-AAD. Pictures were taken under 200x magnification.

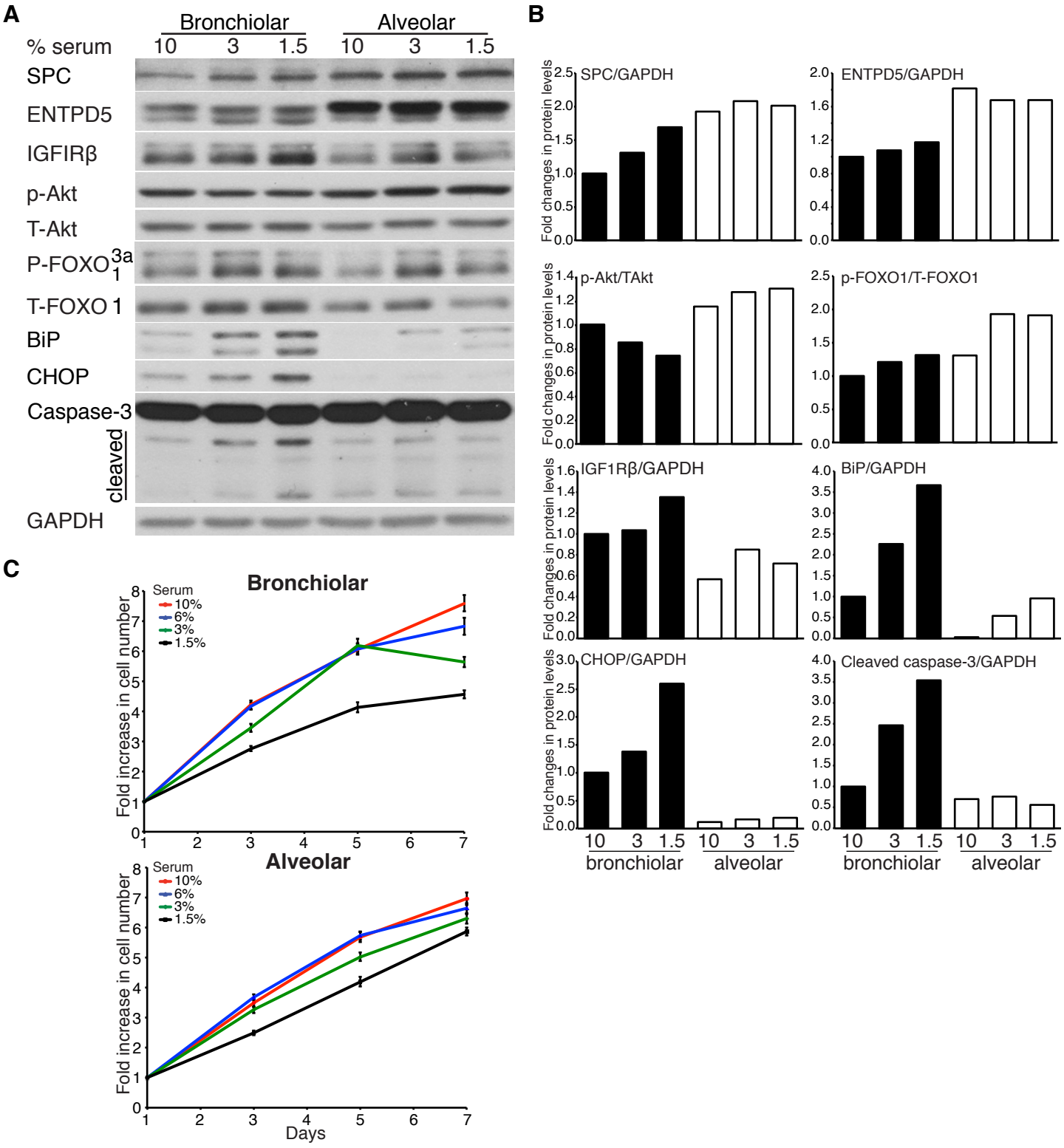

Figure S8: *In vitro* culture of alveolar tumor cells isolated from KPTENp53 mice results in increased ENTPD5 expression and resistance to serum starvation. A, SPC, ENTPD5, IGF1Rβ, phospho-S473 Akt, total Akt, phospho-T24/T32 FOXO1/3a, total FOXO1, BiP, CHOP, caspase-3 (total and cleaved) and GAPDH protein levels in bronchiolar and alveolar KPTENp53 cell lines, grown in the presence of 10%, 3% or 1.5% serum for 72 hours. **B**, Graphs representing quantified protein levels (obtained by ImageJ) assayed for in (**A**). **C**, Proliferation curves of bronchiolar and alveolar KPTENp53 cell lines grown in the presence of 10%, 6%, 3% or 1.5% serum for 7 days (n=6). Data are means ± S.E.M. (**A**) and (**C**) are representative of at least two independent experiments.

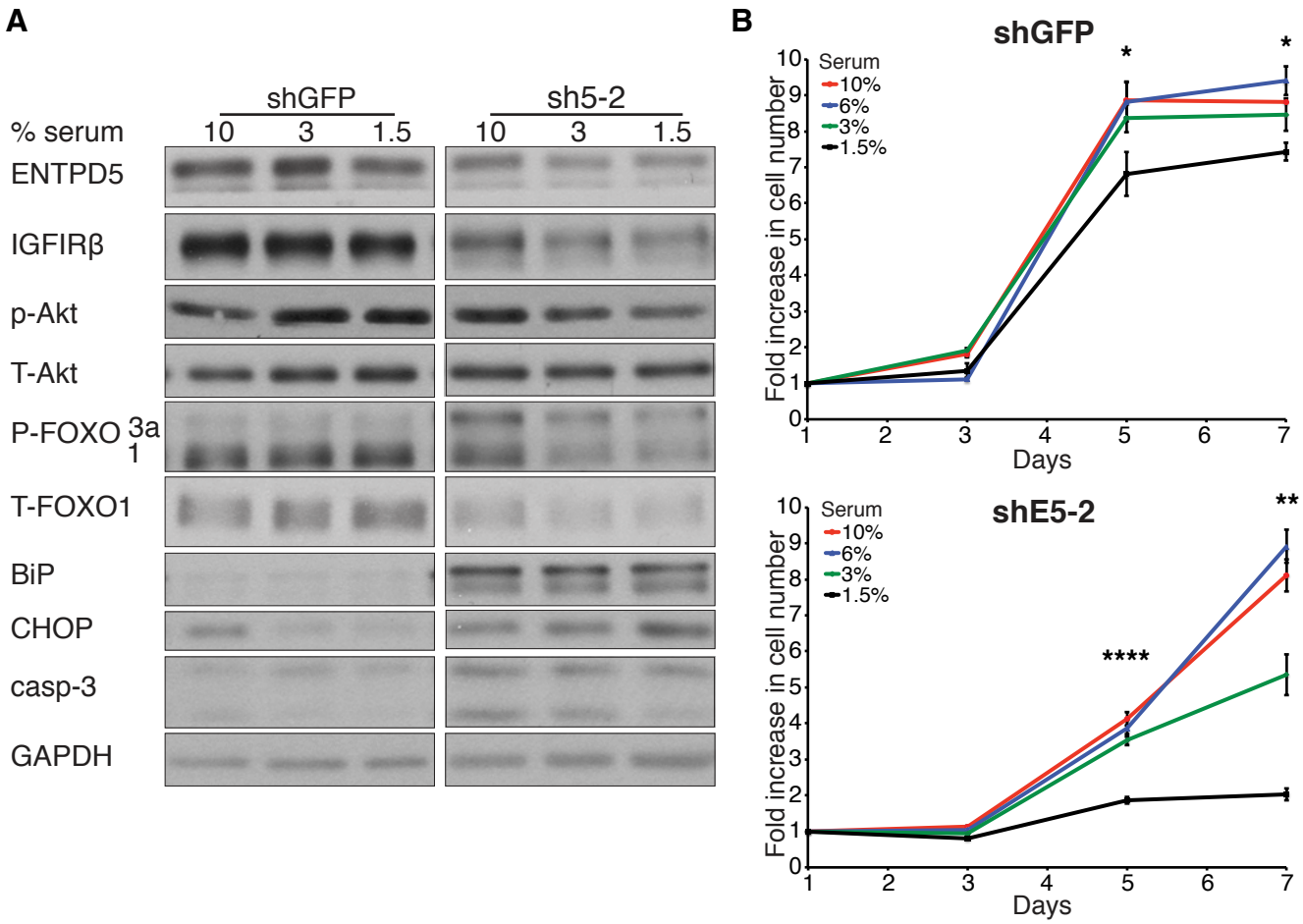

Figure S9: ENTPD5 modulates sensitivity to serum and growth factor receptor levels in KPTENp53 bronchiolar tumor cells. **A**, Effect of *ENTPD5* knockdown using shE5-2 (a hairpin distinct from shE5-1 used in Fig. 4), compared to control *GFP* knockdown, on protein levels of ENTPD5, IGF1Rβ, phospho-S473 Akt, total Akt, phospho-T24/T32 FOXO1/3a, total FOXO1, BiP, CHOP, cleaved capase-3 (casp-3) and GAPDH in bronchiolar KPTENp53 cell lines grown in the presence of 10%, 3% or 1.5% serum for 72 hours. **B**, Proliferation curves of KPTENp53 cell lines cultured in 10%, 6%, 3% or 1.5% serum for 7 days (n=6). Data are means ± S.E.M.; ANOVA/Bonferroni tests were performed. No significant differences were observed for shGFP cell line proliferation at day 5, except for 10% serum condition compared to 1.5%; and at day 7: 1.5% serum condition compared to all other 3 conditions (*$P< 0.05$). For shE5-2 cell line, at day 5: proliferation in 1.5% serum is significantly different from all other 3 conditions (****$P<0.0001$); at day7: proliferation under all conditions is significantly different from any other condition (**$P< 0.01$) except for 10% versus 6%. (**A**) and (**B**) are representative of at least two independent experiments. In (**A**), separated lanes of individual blots were acquired from a single electrophoresis gel.

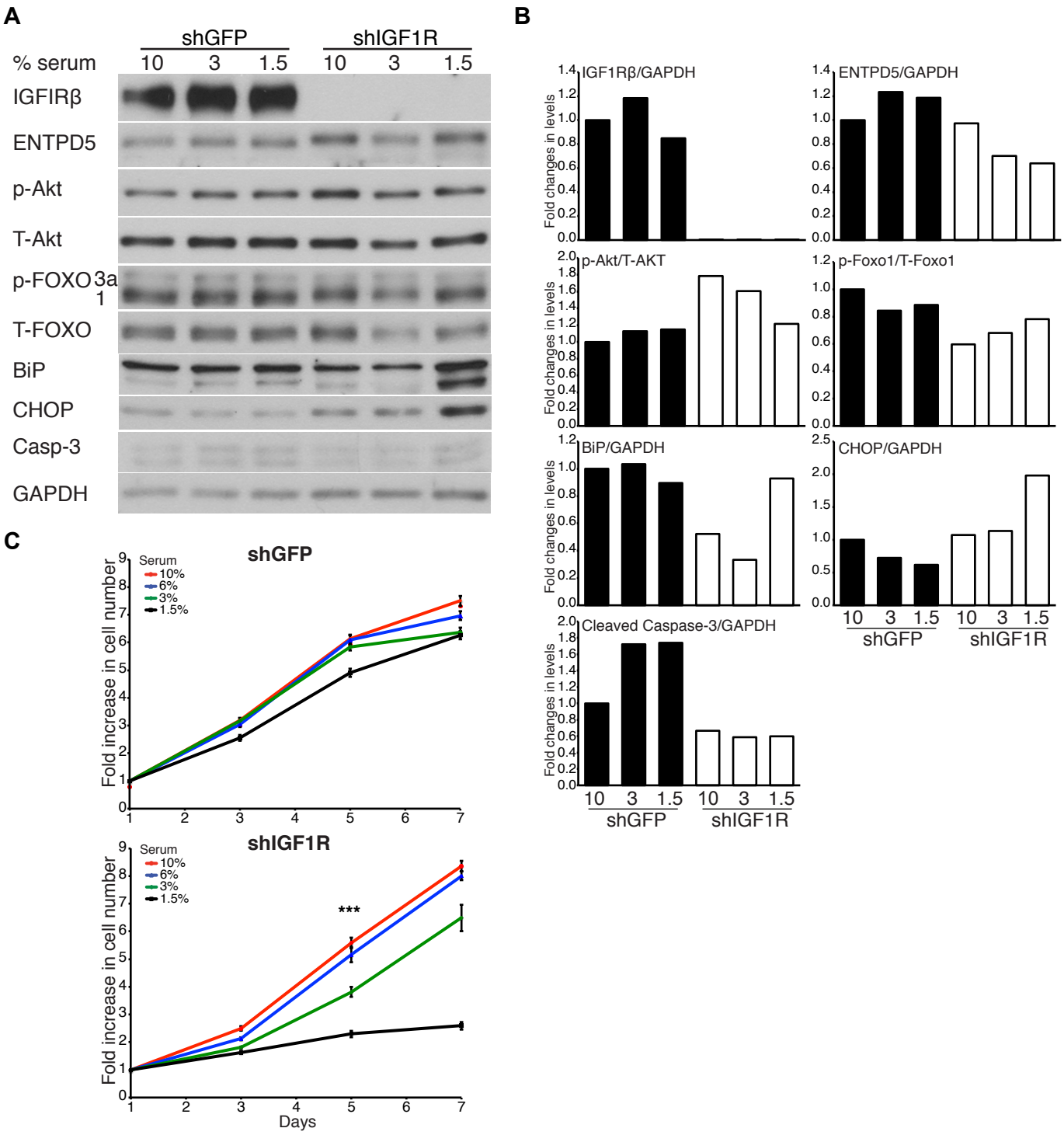

Figure S10: IGF1R levels modulate the sensitivity to serum of KPTENp53 bronchiolar tumor cells. **A**, Effect of knockdown of *IGF1R* (shIGF1R) compared to control *GFP* (shGFP), on protein levels of IGF1Rβ, ENTPD5, phospho-S473 Akt, total Akt, phospho-T24/T32 FOXO1/3a, total FOXO1, BiP, CHOP, cleaved caspase-3 (casp-3) and GAPDH in bronchiolar KPTENp53 cell lines grown in the presence of 10%, 3% or 1.5% serum for 72 hours. **B**, Graphs representing quantified protein levels (obtained by ImageJ) assayed for in (**A**). **C**, Proliferation curves of KPTENp53 cell lines cultured in 10%, 6%, 3% or 1.5% serum for 7 days (n=6). Data are means ± S.E.M.; ANOVA/Bonferroni tests were performed. No significant differences were observed for shGFP cell line proliferation at day 5, except for 1.5% compared to other serum conditions; For shIGF1R cell line, proliferation under all conditions is significantly different from any other condition (***$P < 0.001$) except for 10% versus 6%. (**A**) and (**C**) are representative of at least two independent experiments.

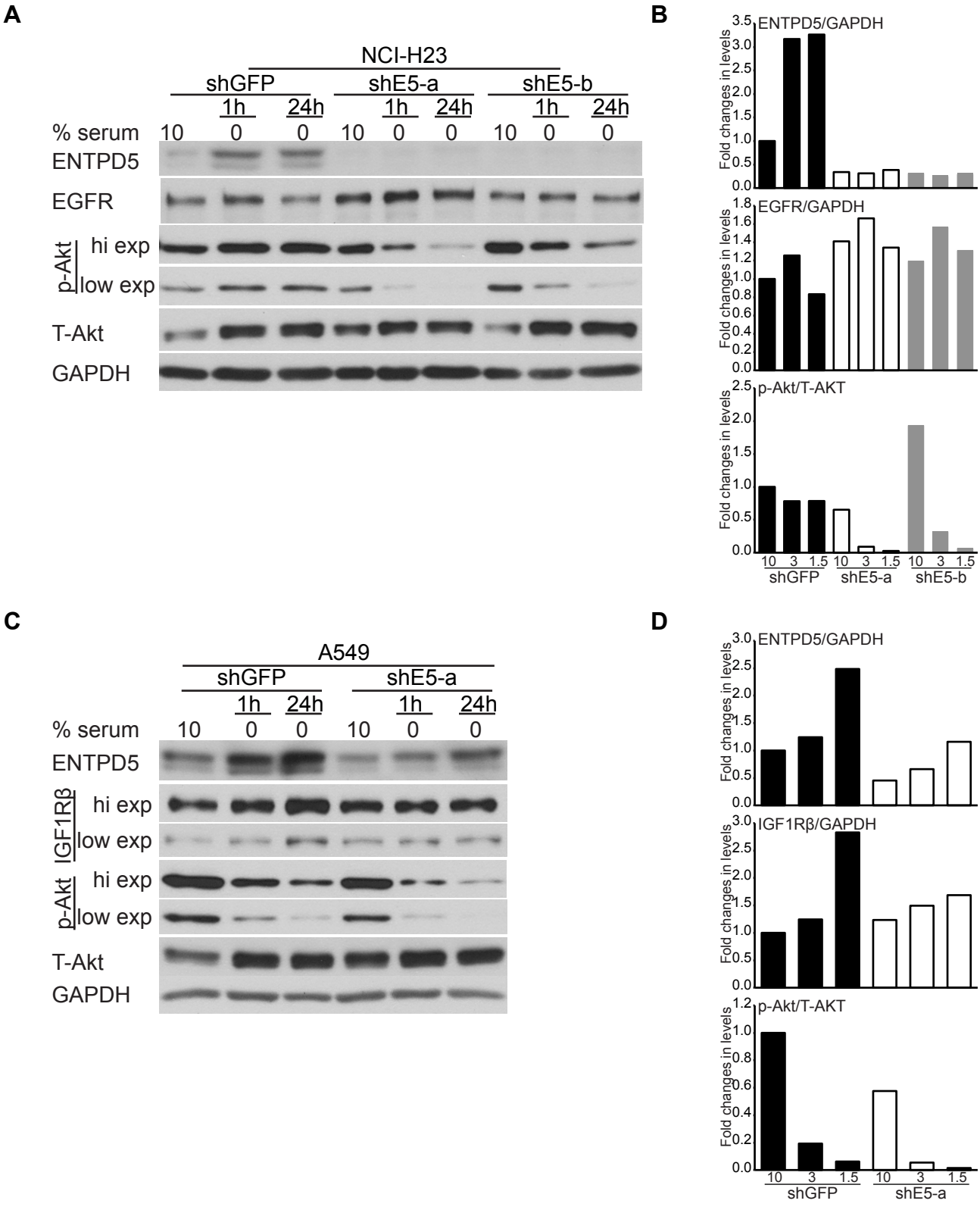

Figure S11: ENTPD5 levels modulate Akt activity in human NSCLC cell lines.
A and **C**, Effect of knockdown of *ENTPD5* using two distinct hairpins (shE5-a and shE5-b) compared to control *GFP* (shGFP), on protein levels of ENTPD5, EGFR, or IGF1Rβ, phospho-S473 Akt, total Akt, and GAPDH in PTEN-low (NCI-H23) (**A**) and PTEN-high (A549) (**B**) NSCLC cell lines, that are grown in the presence of 10% or 0% serum for 1 hour or 24 hours. **B** and **D**, Graphs representing quantified protein levels (obtained by ImageJ) assayed for in (**A**) and (**C**), respectively. (**A**) is representative of two independent experiments.